Preparation and Decomposition of Gold(I) Hydrazido Complexes:[1] Gold Cluster Formation

Visalakshi Ramamoorthy, Zhidan Wu, Yang Yi, and Paul R. Sharp*

Department of Chemistry
University of Missouri—Columbia
Columbia, Missouri 65211

Received September 26, 1991

Metal clusters and their properties continue to attract much interest. Among the metals that form clusters, gold is remarkable in the wide size range, unusual bonding, and lability of the clusters.[2,3] Gold cluster formation and growth has been assumed to occur by aggregation of LAu radicals or small Au(0) clusters such as LAu–AuL presumed to be produced when mononuclear Au(I) complexes are reduced or when larger clusters fragment and recombine.[2a,4] In this paper, we report the isolation of a Au(I) intermediate in the reduction of Au(I) to a gold cluster and present evidence that cluster formation can occur by reductive elimination from Au(I) aggregates brought together by Au(I)–Au(I) interactions.

The reactions of the oxo complex $[(LAu)_3O]BF_4$ **1** (L = PPh_3)[5] with hydrazines and Ph_2NNH_2·HCl (CH_2Cl_2 or THF) are presented in eqs 1–3. With the 1,1-disubstituted hydrazines the initially colorless solutions rapidly turn pale brown, and the hydrazido complexes, $[(AuL)_3NNR_2]BF_4$ **2** (eq 1, R = Me and Ph), are formed. With unsubstituted hydrazine the completely substituted complex $[(AuL)_3NN(AuL)_3](BF_4)_2$ **3** is produced (eq 2), and with the hydrazine hydrochloride, Ph_2NNH_2·HCl, one LAu^+ fragment is consumed in the formation of LAuCl and only two LAu fragments bond to the nitrogen (eq 3).

$$\underset{\mathbf{1}}{[(LAu)_3O]BF_4} + R_2NNH_2 \rightarrow \underset{\mathbf{2}}{[(AuL)_3NNR_2]BF_4} + H_2O \quad (1)$$

$$2\mathbf{1} + N_2H_4 \rightarrow \underset{\mathbf{3}}{[(AuL)_3NN(AuL)_3](BF_4)_2} + 2H_2O \quad (2)$$

$$\mathbf{1} + Ph_2NNH_2{\cdot}HCl \rightarrow \underset{\mathbf{4}}{[H(AuL)_2NNR_2]BF_4} + H_2O + LAuCl \quad (3)$$

The addition of ether to the above reaction mixtures precipitates the air-stable yellow (**2** and **3**) or white (**4**) products, which were characterized by NMR spectroscopy,[6] elemental analyses (**2** (R = Me) and **3**), and X-ray crystal structure determinations[7] (**2** (R = Ph) and **4**).

All of the hydrazido complexes are stable in the solid state. However, solutions (THF of CH_2Cl_2) of **2** (R = Me) are unstable at ambient temperatures and rapidly turn red-brown. The only Au-containing decomposition product is $[(LAu)_6](BF_4)_2$, which can be isolated in a 96% yield.[8] The kinetics of the decomposition in CH_2Cl_2 were examined by ^{31}P NMR spectroscopy and were second order with $k = 0.52 \pm 0.04$ $(M{\cdot}min)^{-1}$ at 22 °C. The organic product from the decomposition is $Me_2NN{=}NNMe_2$,[9,10] giving the net reaction in eq 4.

$$2\underset{\mathbf{2},\ R = Me}{[(AuL)_3NNMe_2]BF_4} \rightarrow [(LAu)_6](BF_4)_2 + Me_2NN{=}NNMe_2 \quad (4)$$

A clue to the nature of this bimolecular decomposition is obtained from the crystal structure of the oxo complex, $[(AuL)_3O]BF_4$ **1**, which we have redetermined in a new crystal form.[11] The complex shows a dimer structure in the solid state (Figure 1) involving interion Au(I)–Au(I) interactions. A similar dimer structure may describe the activated complex in the bimolecular decompositions. The edge-shared bitetrahedral $[(LAu)_6]^{2+}$ cluster is then readily accessible by reductive elimination of $Me_2NN{=}NNMe_2$ and a slight rearrangement of the Au atoms (Scheme I).

Au(I)–Au(I) interactions such as those revealed in the structure of **1** have attracted recent structural and theoretical interest.[12] The importance of these interactions in the reaction chemistry of Au(I) compounds and in cluster formation must be considered on the basis of the above observations. We have observed other reactions which give products probably resulting from similar Au(I)–Au(I) interactions. The CO reaction of **1** and its imido analogues[13] gives the same $[(LAu)_6]^{2+}$ cluster in high yield. While no intermediates are detected, the organic products of these reactions suggest bimolecular pathways. Thus, ureas are formed from the imido compounds (eq 5),[14] and CO_2 and water (eq 6),

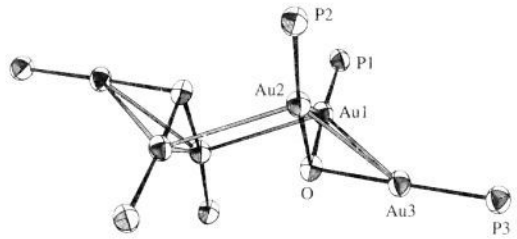

Figure 1. ORTEP plot (phosphine phenyl rings omitted) of $[(AuL)_3O]^+$.

Scheme I

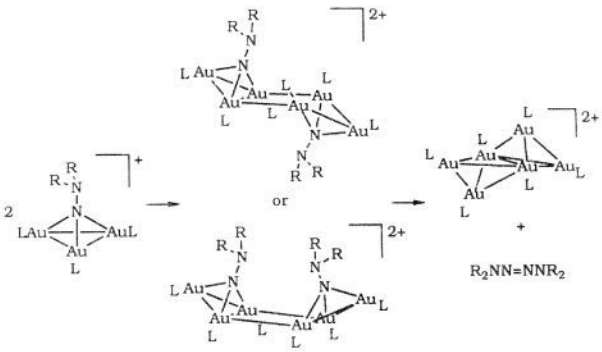

(1) Late Transition Metal μ-Oxo and μ-Imido Complexes. 9. Part 8: Ge, Y.-W.; Sharp, P. R. *Inorg. Chem.*, in press.

(2) For reviews, see: (a) Steggerda, J. J.; Bour, J. J.; van der Velden, J. W. A. *Recl. Trav. Chim. Pays-Bas* **1982**, *101*, 164–170. (b) Hall, K. P.; Mingos, D. M. P. *Prog. Inorg. Chem.* **1984**, *32*, 237–324. (c) Mingos, D. M. P. *Polyhedron* **1984**, *3*, 1289–1297.

(3) Schmid, G.; Pfeil, R.; Boese, R.; Bandermann, F.; Meyer, S.; Calis, G. H. M.; van der Velden, J. W. A. *Chem. Ber.* **1981**, *114*, 3634. Schmid, G. *Struct. Bonding* **1985**, *62*, 51. An alternative formulation for this cluster has been suggested: Fackler, J. P., Jr.; McNeal, C. J.; Winpenny, R. E. P.; Pignolet, L. H. *J. Am. Chem. Soc.* **1989**, *111*, 6434.

(4) Beuter, G.; Strahle, J. *Angew. Chem., Int. Ed. Engl.* **1988**, *27*, 1094–1095.

(5) Nesmeyanov, A. N.; Perevalova, E. G.; Struchkov, Y. T.; Antipin, M. Y.; Grandberg, K. I.; Dyadchenko, V. P. *J. Organomet. Chem.* **1980**, *201*, 343–349.

(6) ^{31}P NMR (CD_2Cl_2): **2** (R = Me), 29.2; **2** (R = Ph), 28.7; **3**, 34.0; **4**, 29.9. ^1H NMR (CD_2Cl_2): **2** (R = Me), 2.82 (s, CH_3), 7.48–7.25 (m, Ph); **2** (R = Ph), 6.85–7.45 (m, Ph); **4**, 6.41 (s, NH), 7.13–7.55 (m, Ph). IR (mull, cm^{-1}): **4**, 3267 m (ν_{NH}).

(7) Crystals of **2**·2THF from THF/ether are monoclinic ($P2_1/n$) with a = 13.854 (3) Å, b = 32.331 (4) Å, c = 15.590 (3) Å, β = 92.216 (19)°, V = 6978.1 (22) Å^3, d_{calcd} = 1.705 g/cm^3, and Z = 4. Crystals of **4**·CH_2Cl_2 from CH_2Cl_2/ether are monoclinic (Cc) with a = 14.376 (6) Å, b = 17.185 (3) Å, c = 19.408 (7) Å, β = 95.840 (20)°, V = 4770 (3) Å^3, d_{calcd} = 1.892 g/cm^3, and Z = 4. Details are available in the supplementary material.

(8) Previous preparations gave low yields: Briant, C. E.; Hall, K. P.; Mingos, D. M. P. *J. Organomet. Chem.* **1982**, *229*, C5.

(9) Identified by GCMS, ^1H NMR, and UV–vis spectroscopy: Madgzinski, L. J.; Pillay, S.; Richard, H.; Chow, Y. L. *Can. J. Chem.* **1978**, *56*, 1657–1667.

(10) Renouf, E. *Ber.* **1880**, *13*, 2169–2174. Watson, J. S. *J. Chem. Soc.* **1956**, 3677–3679.

(11) Crystals of **1**·1.5CH_2Cl_2 from CH_2Cl_2/ether are monoclinic ($P2_1/c$) with a = 14.723 (3) Å, b = 14.808 (3) Å, c = 25.999 (3) Å, β = 104.06 (3)°, V = 5498.3 (17) Å^3, d_{calcd} = 1.946 g/cm^3, and Z = 4. Details are available in the supplementary material.

(12) (a) Jones, P. G. *Gold Bull.* **1981**, *14*, 102, 159; **1983**, *16*, 114; **1986**, *19*, 46. (b) Schmidbaur, H. *Gold Bull.* **1990**, *23*, 11.

(13) Ramamoorthy, V.; Sharp, P. R. *Inorg. Chem.* **1990**, *29*, 3336.

0002-7863/92/1514-1526$03.00/0

believed to derive from H_2CO_3, are formed from **1**.[15]

$$2[(LAu)_3NPh]BF_4 \xrightarrow[CH_2Cl_2 \text{ or } THF]{CO} [(LAu)_6](BF_4)_2 + (PhNH)_2CO \quad (5)$$

$$2\,\mathbf{1} \xrightarrow[CH_2Cl_2 \text{ or } THF]{CO} [(LAu)_6](BF_4)_2 + CO_2 + H_2O \quad (6)$$

Solutions of **2** (R = Ph), **3**, and **4** are much more stable than those of **2** (R = Me), but they also decompose. The kinetics of these and other decompositions will be the subject of future studies directed at understanding the factors that determine the stability of the $[(LAu)_mX]^{n+}$ complexes.

Acknowledgment. We thank ARCO Chemical Company, the Division of Chemical Sciences, Office of Basic Energy Sciences, Office of Energy Research, U.S. Department of Energy (Grant No. DE-FG02-88ER13880) for support of this work, Dr. C. Barnes for assistance with the X-ray work, and the National Science Foundation for partial funding of the X-ray (CHE-9011804) and NMR (PCM-8115599) equipment.

Supplementary Material Available: Listings of kinetic data and details of the structure determinations (27 pages); tables of observed and calculated structure factors (33 pages). Ordering information is given on any current masthead page.

(14) The same results are obtained in MeOH, eliminating the possibility of free PhNCO involvement.
(15) Ureas were obtained in a related Rh system: see ref 1.

Transition-State Structural Features for the Association of Metalloproteases with Phosphorus-Containing Inhibitors

Maria Izquierdo-Martin and Ross L. Stein*

Department of Enzymology, R80N-A54
Merck, Sharp, and Dohme Research Laboratories
P.O. Box 2000, Rahway, New Jersey 07065

Received October 31, 1991

Many enzyme inhibitors reversibly combine with their targeted enzymes with second-order rate constants that are orders of magnitude lower than the diffusion limit.[1] In most cases, however, the reaction step that rate-limits these associations is unclear. We now report results of a study that probes the rate-limiting step for the association of the bacterial metalloprotease TLN[2,3] with phosphoramidon,[4] *N*-((α-L-rhamnopyranosyloxy)hydroxyphosphinyl)-Leu-Trp (**1**), and the human matrix metalloprotease SLN[5-7] with the peptide phosphonamidate, phthalimido-$(CH_2)_4$P(O)(O^-)-Ile-Nal-$NHCH_3$ (**2**).[8]

For both enzyme/inhibitor pairs, progress curves for substrate hydrolysis in the presence of inhibitor are characterized by an initial velocity, v_0, that slowly decays to the final, steady-state

Scheme I. Kinetic Mechanism for Slow-Binding Inhibition of Thermolysin and Stromelysin

$$E + I \underset{k_{off}}{\overset{k_{on}}{\rightleftharpoons}} E{:}I$$

velocity, v_s, with a first-order rate constant, k_{obsd}. Estimates of these three parameters were obtained by fitting the progress curves to the standard equation for slow-binding inhibition:[1]

$$[\text{product}] = v_s t + \left(\frac{v_0 - v_s}{k_{obsd}}\right)[1 - \exp(-k_{obsd} t)] \quad (1)$$

In both cases, the dependencies of v_0, v_s, and k_{obsd} on inhibitor concentration are unexceptional (data not shown) and show that (i) v_0 is independent of inhibitor concentration and equals the control velocity determined in the absence of inhibitor; (ii) v_s is dependent on inhibitor concentration according to eq 2; and (iii) k_{obsd} is linearly dependent on inhibitor concentration. These

$$v_s = \frac{v_0}{1 + \dfrac{[I]}{K_i}} \quad (2)$$

observations support the simple mechanism of Scheme I. According to this mechanism, the linear dependence of k_{obsd} on inhibitor concentration is described by eq 3. The dissociation constant, K_i, is therefore expressed as the simple relationship of eq 4. Note that these experiments were all conducted under the

$$k_{obsd} = k_{on}[I] + k_{off} \quad (3)$$

$$K_i = \frac{k_{off}}{k_{on}} \quad (4)$$

condition $[S] \ll K_m$ (see footnote *a* of Table I for a description of the conditions). This allows us to use the substrate concentration independent eqs 2-4.

K_i, k_{on}, and k_{off} can be estimated from rearranged forms of eqs 2-4 as shown below:

$$K_i = \frac{[I]}{\dfrac{v_0}{v_s} - 1} \quad (5)$$

$$k_{on} = \frac{k_{obsd}}{[I] + K_i} \quad (6)$$

$$k_{off} = k_{on} K_i \quad (7)$$

In practice, a progress curve is analyzed according to eq 1 to obtain best-fit values for v_0, v_s, and k_{obsd}. K_i is then calculated from eq 5 and used together with eq 6 to calculate k_{on}. Finally, k_{off} is estimated as $k_{on}K_i$. Table I summarizes values for these parameters.

To explore transition-state structural features for these reactions, we determined values of $^Dk_{on}$, which, for both reactions, are large and normal (see Table I). For TLN and **1**, the proton inventory[9,10] for k_{on} was also determined and is "dome-shaped" (Figure 1). While several mechanisms can produce "dome-shaped" proton inventories,[10-12] previous studies with TLN[13-15] eliminate many

(1) Morrison, J. F.; Walsh, C. T. *Adv. Enzymol. Relat. Areas Mol. Biol.* **1988**, *61*, 201-301.
(2) Abbreviations: TLN, thermolysin; SLN, stromelysin; Nal, 3-(β-naphthyl)-L-alanine; FA, 3-(2-furyl)acryloyl; DNP, 2,4-dinitrophenyl; $^Dk_{on}$, solvent deuterium isotope effect on k_{on}; $^Dk_{off}$, solvent deuterium isotope effect on k_{off}, $^DK_{assoc}$, solvent deuterium isotope effect on K_{assoc}.
(3) Morihara, K. *Annu. Rev. Biochem.* **1971**, *41*, 179-243.
(4) Kitagishi, K.; Hiromi, K. *J. Biochem.* **1984**, *95*, 529-534.
(5) Matrisian, L. M. *Trends Genet.* **1990**, *6*, 121-126.
(6) Harrison, R.; Teahan, J.; Stein, R. *Anal. Biochem.* **1989**, *180*, 110-113.
(7) Teahan, J.; Harrison, R.; Izquierdo, M.; Stein, R. L. *Biochemistry* **1989**, *28*, 8497-8501.
(8) **2** was designed and synthesized by Dr. Richard Galardy (University of Kentucky) as an inhibitor of human collagenase and was purchased from Elastin Products, Pacific, MO.
(9) Schowen, K. B.; Schowen, R. L. *Meth. Enzymol.* **1982**, *87*, 551-606.
(10) Quinn, D. M.; Sutton, L. D. In *Enzyme Mechanism Isotope Effects*; Cook, P. F., Ed.; CRC Press: Boston, 1991; pp 73-126.
(11) Stein, R. L.; Strimpler, A. M.; Hitoshi, H.; Powers, J. C. *Biochemistry* **1987**, *26*, 1305-1314.
(12) Stein, R. L. *J. Am. Chem. Soc.* **1985**, *107*, 6039-6043.
(13) Izquierdo-Martin, M.; Stein, R. L. *J. Am. Chem. Soc.* **1992**, *114*, 325-331.
(14) Izquierdo, M.; Stein, R. L. *J. Am. Chem. Soc.* **1990**, *112*, 6054-6062.
(15) Stein, R. L. *J. Am. Chem. Soc.* **1988**, *110*, 7907-7908.

0002-7863/92/1514-1527$03.00/0